

Evaluation of Inhomogeneity Correction Performed by Radiotherapy Treatment Planning System

Suman Kumar Putha¹, Dilson Lobo², Holla Raghavendra³, Challapalli Srinivas^{2*}, Sourjya Banerjee², M S Athiyamaan², Johan Sunny K², Abhishek Krishna²

Abstract

Background: Aim of this study is to evaluate the efficacy of inhomogeneity corrections calculated by radiotherapy treatment planning system (TPS) using various densities of materials. **Materials and Methods:** Gammex Computed tomography electron density inserts (EDI's; 14 no's) were used to generate the CT to ED curve with high speed GE CT scanner by noting down the respective HU values of each rod. Treatment plans were generated in XiO TPS with three inhomogeneous phantoms (comprising combination of water, lung and bone equivalent slabs) with different field sizes and for EDI (8 no's) inserted in slots of acrylic tray and validation was carried out using 2D array detector with 20cm×20cm field size for 200 MU. Point dose and fluence measurements were carried with inhomogeneous phantoms combinations and EDI's (placed on the locally fabricated box filled with water medium). **Results:** The mean percentage deviations with standard deviation of calculated point doses against measured ones obtained with 2D array detector at iso-center plane for all three inhomogeneous phantom combinations were found to be -1.13%±0.13%, -3.51%±0.14% and -0.63%±0.27% respectively. On point doses measured under each individual EDI, over all percentage deviation with standard deviation observed is -2.04% ± 1.1%. **Conclusion:** The described method can be implemented in any newly established radiotherapy department as a routine quality measure of TPS to verify its efficacy in performing of inhomogeneity calculation.

Keywords: Dose calculations with inhomogeneity- dose validation- quality assurance of TPS

Asian Pac J Cancer Prev, 23 (12), 4155-4162

Introduction

Human body is made up of various tissues and cavities with varying physical and radiological properties, the most important of which are the lungs, oral cavities, teeth, nasal passages, sinuses, and bones in terms of radiation dosimetry. Tissue inhomogeneity affects the radiation dose distribution, and as external beam radiotherapy (EBRT) treatments become more conformal, the risk of a geographic miss due to insufficient isodose coverage around the target increases (AAPM report 85., 2004). Modern techniques, such as intensity modulated radiotherapy (IMRT), not only require an accurate dose calculation algorithm, such as the Monte Carlo, but also rely on the accuracy of Hounsfield Unit (HU) calibration prior to dose calculations for inhomogeneity corrections (especially in lung cases). Kilo voltage (kV) computed tomography (CT)-based inhomogeneity correction begins with accurate CT to HU calibration, which also requires the accuracy of HU versus electron density (ED)

curves. For each CT scanner, the HU for each kV should be correctly calibrated (Huaiqun Guan et al., 2002). It is recommended to verify that the CT numbers (image grayscale value) to Hounsfield number to relative electron density conversion are performed correctly, since the conversion may be scanner dependent (Andreo et al., 2004). The use of inhomogeneity corrections for tissue density variations has become standard practice in most radiation therapy departments that have direct access to CT scanning for treatment planning system (TPS) of radiation therapy (Huaiqun Guan et al., 2002).

While this is no longer generally the case, it is still important for the user to ensure that the CT numbers fed into the TPS are correctly understood and that there are no calibration offsets. CT scanners are typically calibrated with air and water values; the conversion of CT numbers to relative electron density values is determined by the tissue's atomic number (Huaiqun Guan et al., 2002). Because CT values are dependent on individual scanner parameters such as kVp/filtration and reconstruction

¹Department of Radiation Oncology, MGM Cancer Institute (Unit of MGM Healthcare Pvt Ltd.), Chennai, India. ²Department of Radiation Oncology, Kasturba Medical College (A Constituent Institution of Manipal Academy of Higher Education), Mangalore, Karnataka, India. ³Department of Radiation Oncology, Ruby Hall Clinic, Pune-411001, Maharashtra, India. *For Correspondence: challapalli.srinivas@manipal.edu

algorithm, the CT-to-density conversion curve must be determined empirically (Saw CB et al., 2005). Several reports have emphasized the importance of quality assurance (QA) for TPS since its inception (IAEA, 2004; Fraass B et al., 1998; Möller T. R et al., 1987; Dyk J et al., 1993). According to H Guan et al., (Guan Huaqun et al., 2002), the Kilo-Voltage CT correction is based on precise CT HU calibrations as well as the accuracy of the ED versus HU curves. The following are the objectives of the current work:

a. To generate the CT to ED table using electron density inserts (EDI's) of varying densities with the existing GE CT machine for dose calculations in CMS XiO TPS.

b. To validate the fluence and point doses estimated by TPS with 2D array detector using three types of inhomogeneous phantoms having water equivalent slab, lung, and bone equivalent materials and (EDI's) respectively.

Material and Methods

a) Generation of CT to ED values with EDI's

The electron density (epw) of various tissues and their corresponding CT number in HU were determined using 14 EDI's (Gammex, Inc. Middleton, Wisconsin, USA). The diameter and length of each insert is 3 cm and 8 cm respectively. This data can be assigned to the TPS to ensure accurate calculations of dose distributions under tissue inhomogeneity conditions. An acrylic tray of dimensions 30cm (length) × 30cm (breadth) × 1cm (width) with 16 slots to hold the various EDI's is prepared locally and were inserted in all the slots except in slot numbers 10 and 12. The tray was positioned vertically in the center of water phantom [having dimensions 30cm (length) × 30cm (breadth) × 30cm (width)]. The perspective view of schematic representation of water phantom with try holding EDI's in to the slots. Serial CT images of water phantom along the axial plane of inserts was acquired under CT unit (Model: GE High Speed, GE Medical Systems, Wisconsin, USA) with exposure parameters of 120 kVp and 180 mAs. Figure 1 shows the setup of water phantom having slotted tray with EDI's in position under CT machine to acquire images. From the obtained axial CT images, the HU values of corresponding EDI's were noted as well CT to ED values were tabulated.

b) Validation of fluence and point doses calculated by TPS with 2D array detector

i) Linear accelerator (Linac)

The radiation source used in this study was a 6 MV medical linear accelerator (Model: Compact, Elekta Ltd., Crawley, UK), equipped with an 80 leaf double focus multi leaf collimator, having 100 cm source to axis distance. This machine operates with a dose rate of 350 MU/min (which is the pulse rate used in clinical practice) was calibrated to deliver 1 cGy/MU at iso-center for a field size of 10 cm × 10 cm.

ii) Computerized treatment planning system (TPS)

Computerized TPS (CMS XiO, Elekta Ltd, UK,

version 5.10) having Clarkson, Convolution, superposition (SP), and fast superposition (FSP) algorithms was commissioned with linac beam data measurements and was used to test the accuracy of its dose calculations. The TPS was fed the tabulated CT to ED values, and the superposition algorithm was chosen for dose calculations for better inhomogeneity correction, which was routinely used in clinical practice as a departmental protocol.

iii) Validation of estimated fluence by TPS with 2D array detector using phantoms having inhomogeneous medium

To validate the efficacy of dose calculations under inhomogeneity conditions calculated by TPS using obtained CT to ED data, three (A, B and C) phantoms were created by interweaving 'cork sheets' (30cm × 30cm × 1.2 cm; individual sheet size) of density $\rho=0.23\text{g/cm}^3$ (to simulate lung) and Teflon sheets (30cm × 30cm × 1cm; individual sheet size) of density $\rho\approx 1.6\text{g/cm}^3$ (to simulate bone) in 'RW3solid water' (IBA Dosimetry, Germany) sheet of density $\rho=1.045\text{g/cm}^3$ (30cm × 30cm × 1cm; individual sheets size). Two dimensional array detector (I'mrt MatriXX, M/s IBA Dosimetry, Germany) was used to compare the estimated point doses and dose fluence done by TPS with these phantoms. The detector was calibrated against the calibrated farmer type ionization chamber (Model: FC65-G, IBA Dosimetry, Germany) at Dmax for 1cGy/MU for 6 MV photon beam. The phantoms were placed above the detector which was backed up by 5 cm water equivalent sheets and were scanned under CT. Table 1 represents the three inhomogeneous phantom combinations along with the 2D array detector backed up by the 5 solid water sheets. Serial transverse CT images were imported to TPS from Focal Sim Contouring Station (M/s Elekta Ltd., Crawley, UK) via digital imaging and communications in medicine (DICOM) network.

Dose calculations were performed using SP algorithm (with heterogeneity correction ON) by placing the beam iso-center at the 2D detector plane with 5, 10, 15 and 20 cm² field sizes and treatment plans were generated. We have validated the dosimetric performance of available algorithms and in our earlier study (Kumar et al., 2018). To increase the dosimetric accuracy, a grid size of 2 mm was employed for dose estimates in TPS, as advised by many authors.

Normalization of dose was done at isocenter to an absolute dose of 200 cGy. The calculated point doses at isocenter under these three inhomogeneous phantom combinations for all field sizes were noted. The TPS calculated fluence maps (at isocenter) of corresponding phantoms were exported to Omnipro I'mRT (version 1.7b, IBA Dosimetry, Germany) software for comparison with the 2D array detector. Figure 2 illustrates the execution of treatment plans under linac, with three inhomogeneous phantoms placed above the 2D array detector for point dose and fluence comparison with the TPS estimated ones.

iv) Validation of point dose verification under EDI's estimated by TPS using 2D array detector

In order to represent the situation while the beam passes through an inhomogeneous density, EDI's were inserted vertically in a slotted tray from position 1 to 8,

as shown schematically in figure 3a which depicts the manufacturer's density for each material. These values are taken into account while creating the CT to ED curve in the treatment planning system. This arrangement was placed horizontally in a water filled acrylic box having dimensions of 30cm (length) × 30cm (breadth) × 8cm (height). Water equivalent Super flab gel bolus sheet [20cm (length) × 20cm (breadth)] of 1.5 cm thickness was kept on top of box for adequate dose buildup for 6 MV photon beam and then backed up by four solid water slabs. This combination was kept on top of 2D array detector which is backed up by 5 solid water sheets as shown in the schematic diagram figure 5. The selection of only 8 inserts (shown in figure 3b) placement is because of the limitation of the active area of 2D array detector which is about 24cm (length) × 24cm (breadth).

Transverse CT acquisition of this arrangement (shown in figure 5) was acquired and the scanned serial CT images were transferred to Focalsim contouring station via DICOM network. Contouring of each EDI was done in all transverse slices. The contouring was extended up to the level of 2D array detector plane to locate the position of each EDI at the level of detector plane. Contoured images were exported to TPS for dose calculations using SP algorithm by placing a single open field with a field size of 24cm × 24cm choosing the isocentre at the center of the 2D array detector. The dose was normalized to absolute value at the isocenter for 300 MUs delivery and a treatment plan was generated. The point doses at the center of each EDI at the level of detector plane were noted from the TPS. Figure 4 shows the TPS window of I'mrt MatriXX device with EDI's and iso-dose coverage in transverse, coronal, sagittal planes and anterior field beam's eye view. Figure 5 depicts the setup for measuring point doses and fluence with EDIs kept inside an acrylic box filled with water and placed on an I'mrt MatriXX device under linac.

Results

Table 2 represents the HU values of the corresponding

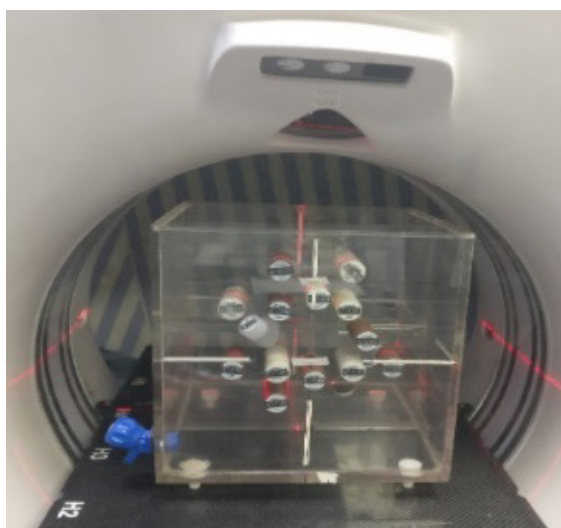


Figure 1. Scanning Setup of Water Phantom Having Slotted Tray with EDI's in Position under CT Machine.

EDI's obtained from scanned CT image which were fed into TPS to generate the CT to ED curve for dose calculations in this work. The table 3 shows the percentage deviations of calculated point doses against measured ones for all field sized used which were obtained with 2D array detector at isocenter for all three inhomogeneous phantom combinations A, B & C. It can be noted that the mean percentage deviations with standard deviation from the calculated doses from these phantom combinations A, B and C are $-1.13\% \pm 0.13\%$, $-3.51\% \pm 0.14\%$ and $-0.63\% \pm 0.27\%$ respectively. However, the deviations for combination B which contains lung (cork sheets) and water equivalent (Solid water sheets) are exceeded more than -3.5% . Figure 6 displays the screenshots of comparison of profiles (for field sizes 5, 10, 15 and 20 cm²) obtained from TPS and 2D array detector with inhomogeneous phantom A as an example. Table 7

Table 1. Inhomogeneous Phantoms A, B & C (Combination of Water, Lung and Bone Equivalent Sheet) with 2D array detector (I'mrt MatriXX) for validation of fluence estimated by TPS.

SN	Material*	Number of sheets		
		A	B	C
1	Water ^{a)}	3	5	8
2	Lung ^{b)}	5	5	-
3	Bone ^{c)}	2	-	2
4	Water ^{a)}	1	1	1
5	I'mrt MatriXX device ^{d)}	1	1	1
6	Water ^{a)}	5	5	5

*Dimensions (length × breadth × thickness) with density (ρ) mentioned below; ^{a)} Water (Solid water sheet): 30 cm×30 cm×1 cm ; (ρ ≈ 1.045 g/cm³); ^{b)} Lung (Cork sheet): 30 cm×30 cm×1 cm ; (ρ ≈ 0.28 g/cm³); ^{c)} Bone (Teflon sheet) : 30 cm×30 cm×1 cm; (ρ ≈ 1.60 g/cm³); ^{d)} I'mrt MatriXX device.

Table 2. HU Values of EDIs Obtained from Scanned CT Image

Position Number in the slotted tray	Description of EDI	Electron Density relative to Water (ρ _p ^w)	HU Values
1	Cortical Bone(SB3)	1.69	1225
2	Brain	1.04	29
3	Adipose (AP6)	0.93	-94
4	Bone (CB2-50% Mineral)	1.47	829
5	Muscle	1.02	15
6	Bone (CB2-30% Mineral)	1.28	299
7	True Water	1	-5
8	Breast	0.96	-55
9	Lung (LN-300)	0.29	-737
10	Slot not used	-----	-----
11	Inner Bone	1.09	210
12	Slot not used	-----	-----
13	Liver	1.06	62
14	Bone (B200)	1.1	231
15	Lung (LN-450)	0.44	-575
16	Zero HU Solid water	0.99	-28



Figure 2. Execution of Treatment Plan under Linac for Point Dose and Fluence Measurements with Three (A, B and C) Inhomogeneous Phantoms Using I'mrt MatriXX Device.

Table 3. Point Doses Obtained at Center of Detector Plane for Different Field Sizes. under three (A, B and C) inhomogeneous phantom combinations

Field Size	A			B			C		
	Calculated	Measured	% Dev.	Calculated	Measured	% Dev.	Calculated	Measured	% Dev.
5×5	147	148.6	-1.08	147.3	152.5	-3.41	128.9	129.3	-0.31
10×10	161.7	163.6	-1.16	161	167.2	-3.71	145	146.4	-0.96
15×15	170.6	172.3	-0.99	169.8	175.8	-3.41	154.7	155.8	-0.71
20×20	176.1	178.4	-1.29	175.9	182.3	-3.51	161.2	162.1	-0.56
	Mean ±SD		-1.13 ± 0.13	Mean ±SD		-3.51 ± 0.14	Mean ±SD		-0.63±0.27

represents the correlation coefficient calculated by the OmniPro I'mRT software from these profiles for different field sizes and phantom combinations.

Table 5 shows the percentage deviations calculated point doses against measured doses with 2D array detector under each individual EDI (8 no's). The average percentage deviation with standard deviation is calculated as $-2.04\% \pm 1.14\%$. Figure 7 shows the comparison of generated vs measured fluence maps with 2D array detector along X-direction in top left and bottom left respectively. The profile comparison is shown in right top window with dashed circle for two EDIs (both are bone equivalent of which the electron densities are 1.69 and 1.47 respectively).

Discussion

TPS QA takes precedence in ensuring that the planned dose will be delivered to the patient, assuming that suitable beam modelling is used (McCullough, 1980; Jacky, 1990). When it comes to estimating radio therapeutic doses to tumors and normal tissues that are surrounded by heterogeneities, choosing the right calculation algorithm is critical (Mohammad, 2017; Christopher, 2006; Zaman, 2019).

Many authors have studied TPS and the behavior of their algorithms, including the CMS XiO TPS, by generating various heterogeneities for estimating dose depositions (Kohno Ryosuke et al., 2009; Fernandes

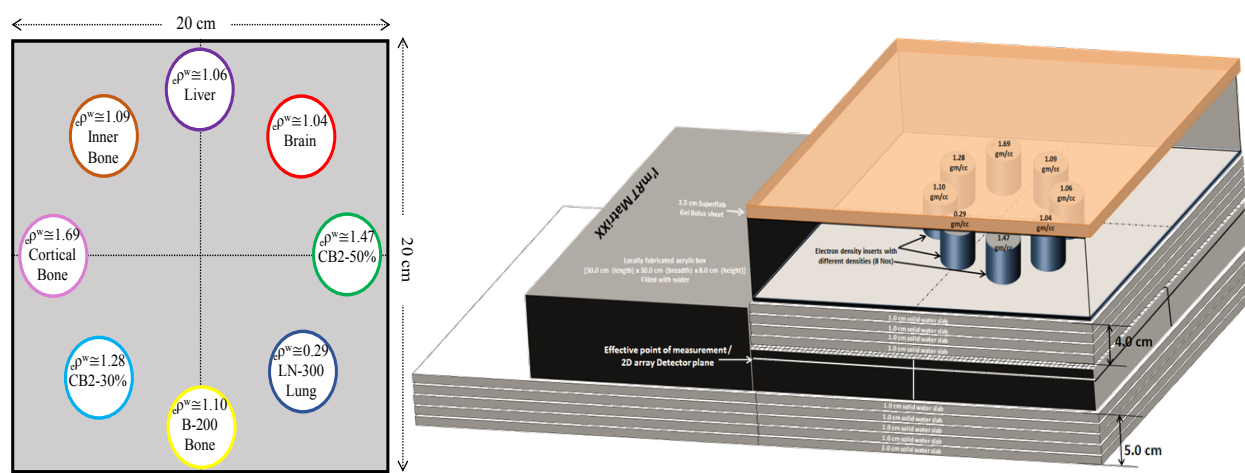


Figure 3. (a) Schematic diagram showing frontal view of the location of 8 EDI's (with epw values relative to water) on an acrylic slotted tray to be fitted in an acrylic box filled with water for fluence and point dose measurements with I'mrt MatriXX device. (b) Schematic diagram showing locally fabricated water filled acrylic box kept on 2D array detector (backed up by 5 solid water plates) having EDI's (8 no's) inserted vertically on slotted tray with 1.5 cm superflab bolus kept on top of box, backed up by 4 nos. solid water sheets.

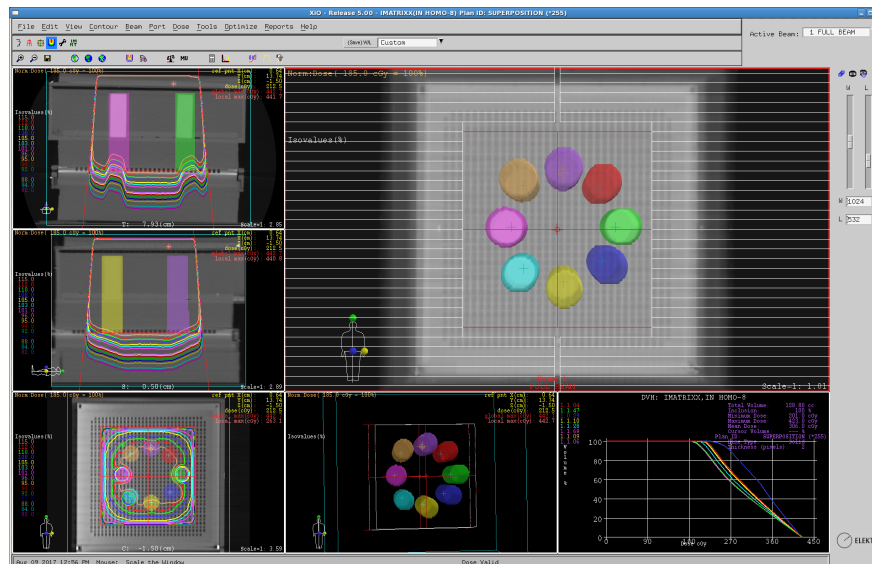


Figure 4. Iso-Dose Coverage around EDI's in the in Transverse, Coronal, Sagittal Planes and Anterior Field Beam's Eye View, 3D View and Dose Volume Histogram Window in XiO TPS.

Table 4. Correlation Coefficient Calculated by the OmniPro I'mRT. software for the TPS generated and acquired profiles by 2D array, detector for three phantom combinations and field sizes.

Phantom Combination	Field Size	Correlation Coefficient
A	5 × 5	0.9828
	10 × 10	0.9924
	15 × 15	0.9924
	20 × 20	0.997
B	5 × 5	0.9942
	10 × 10	0.9978
	15 × 15	0.9973
	20 × 20	0.9961
C	5 × 5	0.9952
	10 × 10	0.9987
	15 × 15	0.9977
	20 × 20	0.996

et al., 2009; Fogliata et al., 2017). Many articles have been published on the dosimetric performance of TPS using commercially available phantoms (e.g., CIRS) and custom built phantoms for the study of the nature of the algorithms (Knöös et al., 2006; Rutonjski Laza et al., 2012; Lu Lanchun et al., 2013; Muralidhar et al., 2009).

The outcome of results obtained in this study on the validity of dose calculations done by CMS XiO treatment planning system (TPS) with I'mrt MatriXX 2D array detector using generated CT to ED data (when the beam passes through differential density combinations of slab phantoms) was found to be $-1.75\% \pm 1.5\%$ (overall percentage deviation with standard deviation) which could be considered as acceptable variation as per TRS-430 (Andreo et al., 2004).

For three phantom combinations and field sizes, the correlation coefficients determined by the OmniPro I'mRT



Figure 5. The Fluence and Point Dose Measurements with EDI's Kept in Water Filled Acrylic Box with I'mrt MatriXX Device under Linac.

software for the TPS generated and acquired profiles by 2D array detector ranged from 0.9828 to 0.9987 (Table 4), which are consistent with the available literature (Shrikant

Table 5. Percentage Deviation of Calculated Point Doses (cGy) vs Measured Ones under each EDI at Detector Plane

EDI (ρ^w)	Calculated	Measured	% Deviation
1.06	213.1	217.1	-1.84
1.04	215.4	219.6	-1.91
1.47	191.1	197.4	-3.19
0.29	261.2	261.8	-0.23
1.1	211.2	218.6	-3.39
1.28	201.7	208.4	-3.21
1.69	186.6	188.7	-1.11
1.09	212.2	215.3	-1.44
Mean ± SD			-2.04 ± 1.14

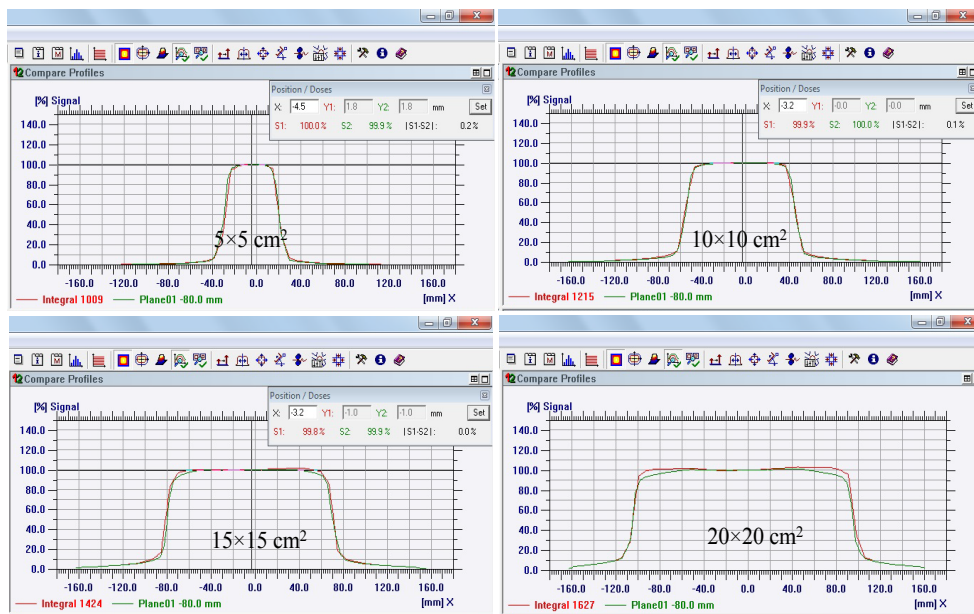


Figure 6. Screenshots of Comparison of Profiles (for field sizes 5, 10, 15 and 20 cm²) Obtained from TPS and 2D Array Detector with Inhomogeneous Phantom A.

Deshpande et al., 2007; Bhangle et al., 2011).

The TPS generated fluence maps were matched to the fluence maps obtained by the 2D array detector with three inhomogeneous phantoms (as illustrated in Figure 8 and 9). For three phantom combinations and field sizes, the correlation coefficients determined by the OmniPro I^mRT software for the TPS generated and acquired profiles by 2D array detector ranged from 0.9828 to 0.9987 (Table 4), which are consistent with the available literature (Shrikant Deshpande et al., 2007; Bhangle et al., 2011). Through fluence maps, the absolute gamma was also valid for all phantom combinations and field sizes.

Apart from the inhomogeneous phantom combinations,

TPS's calculations with EDI's were also tested, and the calculated and measured values with a 2D array detector were found to be consistent. Under all of the inserts, the point dosages were all within 2%. When the heterogeneity correction function was turned on, the measured value under the inserts of bone equivalent materials CB2-30 and B-200 was slightly higher, at -3.21% and -3.39%, respectively which the deviation was in agreement literature (IAEA TECDOC 1583, 2008). In the case of EDIs measured with a 2D array detector, the correlation coefficient was found to be 0.9956. Though the predicted doses from TPS are compared to measurements taken in water, the CT to ED curve is used to manage heterogeneity

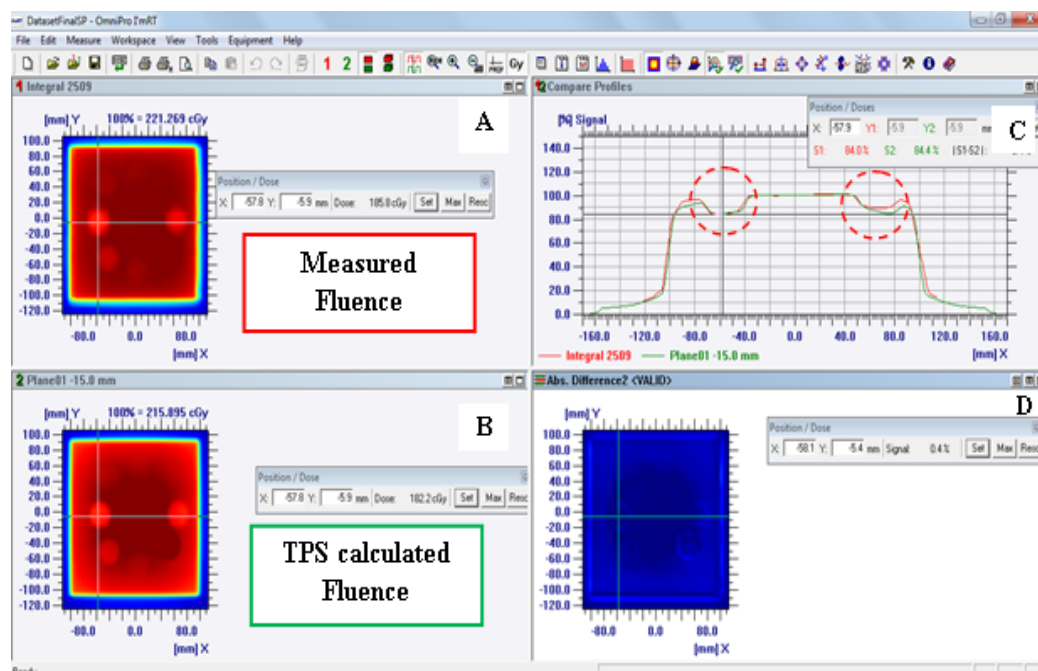


Figure 7. Representative Screen Shot of Comparison of Fluence Obtained from TPS vs Measured with I^mrt MatriXX

adjustments as appropriate.

In conclusion, In this study, the relation between of CT number and electron densities of different EDI is established by measuring the corresponding Hounsfield units. The generated CT to ED table is fed to XiO TPS for regular patient dose calculations. TPS's inhomogeneity corrections are validated using inhomogeneous phantom combinations and EDI's. The achieved results using this methodology ensure the inhomogeneity corrections performed by the treatment planning system for generating complex radiotherapy plans.

Author Contribution Statement

PS and DL were in charge of data collection and manuscript preparation. CS was created by experimentation and literature study. RH was a scientific collaborator in the provision of CT to the ED phantom. SB, AT, JS, and AB are aided in data collecting and paper editing. The final manuscript was reviewed and approved by all authors.

Acknowledgements

Authors would like to express sincere thanks to Mr. Prastuth K and Mr. Ranjith T, Undergraduate students for their active participation this study.

Funding Statement

There was no financial funding involved in this study.

Ethics approval

This study was conducted under the protocol approved by the Institutional Ethics Committee, Kasturba Medical College, Mangaluru (Reg.No.IEC/MLR 11-14/224)

Consent for publication

Author declares that this study was carried out at Department of Radiation Oncology, Kasturba Medical College (A constituent Institution of Manipal Academy of Higher Education), Mangalore, Karnataka, India. All of the authors declare that they have all participated in the design, execution, and analysis of the paper, and that they have approved the final version.

Conflicts of interest

The authors have no conflicts of interest to declare that are relevant to the content of this article.

References

Fernandes A, Jacob K, Rosa MJ, et al (2009). Teixeira. Comparative study of convolution and superposition of the CMS XiO treatment planning system for different locations in radiotherapy. *Radiother Oncol*, **92**, S150.
AAPM Report No. 85. Tissue Inhomogeneity Corrections for Megavoltage Photon Beams. Madison: Medical Physics Publishing, 2004.
Andreo P, Cramb J, Fraass BA, et al (2004). Commissioning and Quality Assurance of Computerized Planning Systems for Radiation Treatment of Cancer. Technical Report Series No. 430. Vienna: International Atomic Energy Agency (IAEA).
Bhangle JR, Sathiyarayanan VK, Kumar NK, Vaitheeswaran

R (2011). Dosimetric analysis of beam-matching procedure of two similar linear accelerators. *J Med Phys*, **36**, 176-80.
Christopher M. Bragg JC (2006). Dosimetric verification of the anisotropic analytical algorithm for radiotherapy treatment planning. *Radiother Oncol*, **81**, 315-23.
Dyk JV, Barnett RB, Cygler JE, Shragge PC (1993). Commissioning and quality assurance of treatment planning computers. *Int J Radiat Oncol Biol Phys*, **26**, 261-73.
Fogliata A, Vanetti E, Albers D, et al (2007). On the dosimetric behavior of photon dose calculation algorithms in the presence of simple geometric heterogeneities: Comparison with Monte Carlo calculations. *Phys Med Biol*, **52**, 1363-85.
Fraass B, Doppke K, Hunt M, et al (1998). American Association of Physicists in Medicine Radiation Therapy Committee Task Group 53: Quality assurance for clinical radiotherapy treatment planning. *Med Phys*, **25**, 1773-1829.
Guan H, Fang FY, Jae HK (2002). Accuracy of inhomogeneity correction in photon radiotherapy from CT scans with different settings. *Phys Med Biol*, **47**, 223.
Huaqun G, Fang-Fang Y, Jae HK (2002). Accuracy of inhomogeneity correction in photon radiotherapy from CT scans with different settings. *Phys Med Biol*, **47**, 223.
IAEA TECDOC 1583 (2008). Commissioning of radiotherapy treatment planning systems: Testing for typical external beam treatment techniques. Vienna: International Atomic Energy Agency.
Jacky J, White CP (1990). Testing a 3-D radiation therapy planning program. *Int J Radiat Oncol Biol Phys*, **18**, 253-61.
Knöös T, Wieslander E, Cozzi L, et al (2006). Comparison of dose calculation algorithms for treatment planning in external photon beam therapy for clinical situations. *Phys Med Biol*, **51**, 5785-807.
Kohno R, Satoshi K, Eriko H, et al (2009). Dosimetric verification in inhomogeneous phantom geometries for the XiO radiotherapy treatment Planning System with 6-MV Photon Beams. *Radiol Phys Technol*, **2**, 87-96.
Kumar PS, Banerjee S, Arun Kumar ES, et al (2018). In vivo dose estimations through transit signal measured with thimble chamber positioned along the central axis at electronic portal imaging device level in medical linear accelerator in carcinoma of the middle-third esophagus patients undergoing three-dimensional conformal radiotherapy. *J Cancer Res Ther*, **14**, 300-7.
Lu L, Guy Y, Jian ZW, et al (2013). A practical method to evaluate and verify dose calculation algorithms in the treatment planning system of radiation therapy. *Int J Med Physics Clin Engin Radiat Oncol*, **1**, 76-87.
McCullough EC, Krueger AM (1980). Performance evaluation of computerized treatment planning systems for radiotherapy: external photon beams. *Int J Radiat Oncol Biol Phys*, **6**, 1599-1605.
Mohammad Taghi BT, Bagher F, Shokouhoman S (2017). Evaluation of dose calculations accuracy of a commercial treatment planning system for the head and neck region in radiotherapy. *Rep Pract Oncol Radiother*, **22**, 420-7.
Möller TR, Rosenow U, Bentley RE, et al (1987). ICRU report 42: Use of computers in external beam radiotherapy procedures with high-energy photons and electrons. *JICRU*, **22**, 65-7.
Muralidhar KR, Narayana PM, Alluri KR, NVNM S (2009). Comparative study of convolution, superposition, and fast superposition algorithms in conventional radiotherapy, three-dimensional conformal radiotherapy, and intensity modulated radiotherapy techniques for various sites, done on CMS XiO planning system. *J Med Phys*, **34**, 12-22.
Mzenda B, Koki VM, Rick S, et al (2014). Modeling and dosimetric performance evaluation of the ray station

- treatment planning system. *J Appl Clin Med Phys*, **15**, 29–46.
- Rutonjski L, Borislava P, Milutin B, et al (2012). Dosimetric verification of radiotherapy treatment planning systems in Serbia: National Audit. *Radiat Oncol*, **7**, 155.
- Saw CB, Loper A, Komanduri K, et al (2005). Determination of CT-to-density conversion relationship for image-based treatment planning systems. *Med Dosim*, **30**, 145-8.
- Senthilkumar S (2014). Design of homogeneous and heterogeneous human equivalent thorax phantom for tissue inhomogeneity dose correction using TLD and TPS measurements. *Int J Radiat Res*, **12**, 179–88.
- Shrikant Deshpande VK, Sathiyarayanan, Janhavi B, et al (2007). Dosimetric and QA aspects of Konrad inverse planning system for commissioning intensity modulated radiation therapy. *J Med Phys*, **32**, 51-5.
- Zaman A, Kakakhel M, Hussain A (2019). A comparison of Monte Carlo, anisotropic analytical algorithm (AAA) and Acuros XB algorithms in assessing dosimetric perturbations during enhanced dynamic wedged radiotherapy deliveries in heterogeneous media. *J Radiother Pract*, **18**, 75-81.



This work is licensed under a Creative Commons Attribution-Non Commercial 4.0 International License.